Cancer Letters 461 (2019) 102–111

Contents lists available at ScienceDirect

Cancer Letters

journal homepage: www.elsevier.com/locate/canlet

Original Articles

Low-dose triple drug combination targeting the PI3K/AKT/mTOR pathway and the MAPK pathway is an effective approach in ovarian clear cell carcinoma

Joseph J. Caumanns[a], Anne van Wijngaarden[a,b], Arjan Kol[a], Gert J. Meersma[a], Mathilde Jalving[b], René Bernards[c], Ate G.J. van der Zee[a], G. Bea A. Wisman[a,1], Steven de Jong[b,*,1]

[a] Department of Gynecologic Oncology, Cancer Research Center Groningen, University Medical Center Groningen, University of Groningen, Hanzeplein 1, 9713 GZ, Groningen, the Netherlands
[b] Department of Medical Oncology, Cancer Research Center Groningen, University Medical Center Groningen, University of Groningen, Hanzeplein 1, 9713 GZ, Groningen, the Netherlands
[c] Division of Molecular Carcinogenesis and Oncode Institute, The Netherlands Cancer Institute, Plesmanlaan 121, 1066 CX, Amsterdam, the Netherlands

ARTICLE INFO

Keywords:
Combination treatment
PI3K/AKT/mTOR
MAPK
PDX models
Ovarian clear cell carcinoma

ABSTRACT

Advanced stage ovarian clear cell carcinoma (OCCC) is poorly responsive to platinum-based chemotherapy and has an unfavorable prognosis. Previous studies revealed heterogeneous mutations in PI3K/AKT/mTOR and MAPK pathway nodules converging in mTORC1/2 activation. Here, we aimed to identify an effective low-dose combination of PI3K/AKT/mTOR pathway and MAPK pathway inhibitors simultaneously targeting key kinases in OCCC to preclude single-inhibitor initiated pathway rewiring and limit toxicity. Small molecule inhibitors of mTORC1/2, PI3K and MEK1/2 were combined at monotherapy IC_{20} doses in a panel of genetically diverse OCCC cell lines (n = 7) to determine an optimal low-dose combination. The IC_{20} dose triple combination reduced kinase activity in PI3K/AKT/mTOR and MAPK pathways, prevented single-inhibitor induced feedback mechanisms and inhibited short and long-term proliferation in all seven cell lines. Finally, this low-dose triple drug combination treatment significantly reduced tumor growth in two genetically characterized OCCC patient-derived xenograft (PDX) models without resulting in weight loss in these mice. The effectiveness and tolerability of this combined therapy in PDX models warrants clinical exploration of this treatment strategy for OCCC and might be applicable to other cancer types with a similar genetic background.

1. Introduction

Ovarian clear cell carcinoma (OCCC) is the second most common epithelial ovarian cancer subtype. Advanced stage OCCC responds poorly to platinum-based chemotherapy and has a worse overall survival compared to the most common ovarian cancer subtype (high-grade serous) [1]. There is an urgent need for targeted treatment strategies. Recent genomic analysis uncovered a heterogeneous mutation- and copy number alteration (CNA) spectrum in OCCC. DNA binding AT-rich interactive domain 1A gene (*ARID1A*), a key subunit of the SWI-SNF chromatin remodeling complex, is deleteriously mutated in 40–57% of OCCC tumors [2–4]. This is the highest frequency among all cancer types and strategies specifically targeting *ARID1A* mutated OCCC are being explored extensively [4–6]. Interestingly, almost no mutations in *TP53* are found in OCCC [4]. The most frequent PI3K/AKT/mTOR related alterations are found in the PI3K catalytic domain encoding subunit *PIK3CA*, which is mutated in 30–40% of OCCC, and the PI3K antagonist *PTEN*, with loss of expression in 40% of OCCC [3,4,7,8]. Other alterations include deleterious mutations in the PI3K regulatory subunit *PIK3R1* and amplifications and mutations in the PI3K downstream effectors *AKT1* and *AKT2* [4,9–11]. MAPK related alterations are primarily found in the oncogene *KRAS*, which is mutated in 5–14% and amplified in 18% of OCCC [3,4,7,11,12]. Occasionally, *NRAS* and *BRAF* mutations have been detected [4,7,9,10]. Additionally, ERBB family of receptor tyrosine kinases amplifications (*EGFR*, *ERBB2* and *ERBB3*) and mutations (*EGFR*, *ERBB2*, *ERBB3* and *ERBB4*) have been described in OCCC [4,9,10,13,14]. Unfortunately, EGFR and EGFR-ERBB2 dual inhibitors did not show efficacy in pretreated non-subtype selected ovarian cancer patients [15–17]. In a recent report we described the heterogeneous genomic landscape of PI3K/AKT/mTOR

* Corresponding author.
E-mail address: s.de.jong@umcg.nl (S. de Jong).
[1] Last two authors share senior authorship.

https://doi.org/10.1016/j.canlet.2019.07.004
Received 22 May 2019; Received in revised form 6 July 2019; Accepted 11 July 2019

and MAPK pathways in OCCC patients and cell lines [4]. Interestingly, we found high mTORC1/2 activity in tumors from OCCC patients compared to this activity in tumors from high-grade serous ovarian cancer patients, and demonstrated high efficacy of mTORC1/2 inhibition in vitro and in vivo [4]. Unfortunately, mTORC1/2 inhibitors have only shown efficacy when used above the maximum tolerated dose in non-OCCC patients, indicating that these inhibitors cannot be administered at therapeutically relevant doses [25,26].

PI3K, mTORC1/2 and MEK1/2 are attractive targets for treatment given the high frequency of mutations present in regulatory proteins and kinases of the PI3K/AKT/mTOR and MAPK pathway in OCCC. Single-targeted and suboptimal inhibition of PI3K, mTORC1/2 or MEK1/2 can result in re-activation of PI3K/AKT/mTOR or MAPK signaling via negative feedback mechanisms or rewiring. For example, inhibition of mTORC1/2 can upregulate the membrane receptor IRS-1 and induce phosphorylation of AKT [18,19]. Moreover, interactions between the PI3K/AKT/mTOR pathway and the MAPK pathway induces cross-activation, complicating sustainable inhibition of both proliferation pathways [20]. Despite the strong reduction in p-S6, reflecting effective mTORC1/2 inhibition, we indeed observed evidence for activation of feedback- or rewiring mechanisms in OCCC models after mTORC1/2 inhibition, suggesting the involvement of PI3K [4].

Dual PI3K-mTOR1/2 inhibitors, e.g. BEZ235 and XL765, exhibit high potency in in vitro models including ovarian cancer but severe toxicity, especially hyperglycemia and gastrointestinal toxicity, was observed in cancer patients at effective PI3K-mTORC1/2 inhibitor dose [21–24]. This may well be related to the important role of PI3K/AKT/mTOR and MAPK pathway signaling in normal tissue. These observations indicate that a careful titration of combined single-targeted inhibitors may result in optimal tumor efficacy with acceptable systemic toxicity.

Therefore, we investigated whether the addition of PI3K or MEK1/2 inhibitors to mTORC1/2 targeting agents, all at low-dose, prevents feedback mechanisms and cross-activation in OCCC, while maintaining antitumor potency. Firstly, we determined the efficacy of PI3K/AKT/mTOR pathway and MAPK pathway inhibitors in a panel of OCCC cell lines reflecting the genetic diversity of OCCC. We tested if low concentrations of the inhibitors demonstrated potentiating interactions in OCCC cell lines. Secondly, we studied the molecular interactions and the cellular consequences of these combinations. Ultimately, two established OCCC patient-derived xenograft (PDX) models were treated with low-doses of the most effective in vitro triple drug combination, i.e. concentrations far below the maximum tolerated doses of single agents in mice, to demonstrate antitumor activity while minimizing systemic toxicity in these mice.

2. Methods

2.1. Cell lines

We obtained seven human OCCC cell lines: RMG1, OVMANA, and HAC2 (JCRB Cell Bank, Japan); JHOC5 (RIKEN Cell Bank, Japan); SMOV2 and KOC7C (Dr. Hiroaki Itamochi, Tottori University School of Medicine, Tottori, Japan) and ES2 (Dr. E. Berns, Erasmus MC, Rotterdam, the Netherlands). All OCCC cells were maintained in RPMI supplemented with 10% fetal calf serum. The non-transformed human retinal pigment epithelial cell line (RPE1) was maintained in DMEM-low medium supplemented with 10% fetal calf serum. All cell lines were tested by STR profiling and tested mycoplasma free. All cells were kept in culture for a maximum of 50 passages.

2.2. Inhibitors

AZD8055, GDC0941, selumetinib and MLN0128 were obtained from Axon Medchem (the Netherlands). ABT-737 was obtained from MedchemExpress (United Kingdom). All inhibitors were dissolved in DMSO and stored at −80 °C.

2.3. MTT assays

Cells were seeded in 96-wells plates and cultured overnight (16–18 h) before 96 h treatment with increasing inhibitor concentrations. Plating concentrations were: ES2, JHOC5 and KOC7C 2000 cells/well, RMG1 and SMOV2 4000 cells/well, HAC2 and OVMANA 6000 cells/well. After 96 h methyl thiazolyl tetrazolium (MTT) was added to a final concentration of 0.5 mg/ml and cells were incubated for four additional hours. Cells were then dissolved in DMSO, and the produced formazan was measured at 520 nm with a Bio-Rad iMark spectrometer. IC_{20} inhibitory concentrations were determined in Graphpad Prism® 6.01.

2.4. Long-term survival assays

Cells were seeded in 12-well plates and cultured overnight (16–18 h) before treatment was added. Plating concentrations were: ES2 500 cells/well, HAC2 5000 cells/well, JHOC5 1000 cells/well, KOC7C 250 cells/well, RMG1 5000 cells/well, SMOV2 5000 cells/well, OVMANA 8000 cells/well and RPE1 500 cells/well. RPE1 cells were treated with AZD8055, GDC0941 and selumetinib concentrations at 25% and 75% of the difference between the lowest and highest IC_{20} from our OCCC cell line panel. After 7–14 days cells were fixed with 4% formaldehyde and stained with 0.1% crystal violet and subsequently scanned.

2.5. Western blotting

Cells were collected with rubber policemen cell scrapers and lysed in M-PER mammalian protein extraction reagent (Thermo Fischer, USA, 78501) containing Halt protease and phosphatase inhibitors (1:100) (Thermo Fischer, USA, 78444). For Western blot primary antibodies against p-AKT^{308} (9275, 1:1000), p-AKT^{473} (9271, 1:1000), p-ERK1/2 (9102, 1:1000), p-S6 (2211, 1:1000), p-4EBP1 (9455, 1:1000), PARP (9532, 1:1000) and Cleaved Caspase-3 (9661, 1:1000) were obtained from Cell Signaling Technology (USA). β-Actin (C4, 1:1000) was obtained from MPbiomedicals (USA). Protein membranes were stained with horseradish peroxidase bound Rabbit anti-Goat and Mouse anti-Rabbit secondary antibodies (DAKO, USA, 1:1000) and visualized on a ChemiDoc MP imaging system (Bio-Rad, USA) with chemiluminescent HRP substrate.

2.6. Apoptosis flow cytometry

Cells were seeded in 6-wells plates and incubated overnight (16–18 h) before treatment was added. Cells were harvested in their own media using trypsine, stained with 1,1′,3,3,3′,3′-hexamethylindodicarbo-cyanine iodide ($DiIC_1$ (5)) dye (Thermo Fischer, USA) for 30 min at 37 °C and subsequently stained with propidium Iodide (Thermo Fischer, USA). At least 10,000 events were measured on a FACS Calibur (Becton Dickinson, USA). $DiIC_1$ (5), a dye that accumulates in mitochondria, is lost when cells undergo apoptosis via the intrinsic apoptosis pathway. By combining the quartiles of cells that were propidium iodide positive or had lost $DiIC_1$ (5) dye, both apoptotic and necrotic cells could be quantified. FlowJo software was used for data analysis. Statistical significance was determined using repeated measures one-way ANOVA with post-hoc Tukey's multiple comparison test.

2.7. Combination treatment in patient-derived xenograft models

All animal experiments were approved by the Institutional Animal Care and Use Committee of the University of Groningen (Groningen, the Netherlands) and carried out in accordance with the approved guideline “code of practice: animal experiments in cancer research”

(Netherlands Inspectorate for Health Protection, Commodities and Veterinary Public Health, 1999). Establishment and studies of PDX models were performed in accordance with the PDX-MI standard [25]. Before surgery, all patients from whom tumor samples were obtained for PDX modeling gave written informed consent for collection and storage of tissue samples in a tissue bank for future research. All relevant patient data were retrieved and transferred into an anonymous, password-protected, database. The patients' identity was protected by study-specific, unique patient codes and their true identity was only known to two dedicated data managers. According to Dutch regulations, these precautions meant no further institutional review board approval was needed (http://www.federa.org/). PDX.180 was derived from tumor material obtained at interval debulking surgery from a 59 year old FIGO stage IIIC OCCC patient treated with neoadjuvant carboplatin/paclitaxel (CP) chemotherapy and deceased 10 months after initial diagnosis with disease. PDX.247 was established from tumor material obtained at primary surgery from a 54 year old FIGO stage IIB OCCC patient, who had a complete debulking followed by CP chemotherapy and no evidence of disease after 29 months of follow-up. Surgical tissues were implanted in NOD.CB17-Prkdcscid/NCrHsd (NSG) mice (internally bred, Central Animal Facility, University of Groningen) and propagated successfully to the F3 or F4 generation according to previously described methods [26]. The PDX models were sequenced for 40 genes, including genes with a high mutation frequency in OCCC, *ARID1A* and other cancer-related genes using *Haloplex custom kit* (Agilent technologies®, USA) [4]. Additional SNP genotyping of the PDX models was performed with *HumanOmniExpressExome-8BeadChip* (Illumina, USA) [4]. F3 or F4 tumor pieces were cut into 3 × 3x3 mm3 sections and subcutaneously implanted in the flank of 12–16 week old NSG mice. Weight, fur quality and overall activity of the mice were monitored at least once per three days. Tumor growth was quantified at least once per three days by caliper measurements according to the formula ($width^2$ x length)/2. Sacrifice criteria included 15% weight loss, tumor size > 1500 mm^3 or prolonged severe overall activity according to the approved guidelines “code of practice: animal experiments in cancer research” (Netherlands Inspectorate for Health Protection, Commodities and Veterinary Public Health, 1999). When tumors demonstrated sustained growth (on average after 27 days), mice were randomized into vehicle control or treatment groups (n = 3–5 mice/group). AZD8055 (4 mg/kg), GDC0941 (30 mg/kg), selumetinib (20 mg/kg) or the combination were diluted in 0.2% Tween-80 0.5% hydroxyl-propyl methylcellulose (Sigma-Aldrich, USA) and administered by oral gavage daily. Treatment with AZD8055, GDC0941, selumetinib, the combination or vehicle was continued for 21 days, after which all mice were sacrificed. One mouse in the selumetinib treated group died on treatment day four due to undefined reasons. In historical data, AZD8055 (10 mg/kg in 10% DMSO, 40% Polyethylene glycol 300) was administered intraperitoneally daily [4]. Relative tumor growth was determined by tumor volume/tumor volume at start of first treatment (day 0). For further analysis the tumors were resected, split into two parts of which one part was snap frozen at −80 °C while the other part was paraffin embedded. Statistical significance for tumor growth was determined using two-way ANOVA with Bonferoni post-hoc test correction in Graphpad Prism® 6.01.

2.8. Immunohistochemical analysis

From paraffin-embedded PDX tumors slices (3 µm thick) were cut using a microtome and placed on 3-aminopropyltriethoxysilane-coated glass slides. Heat-induced antigen retrieval was performed in 10 mM citrate buffer using a 400 W rotary microwave. Endogenous peroxidase was blocked by 30 min incubation with 0.3% H_2O_2 in PBS. Endogenous avidin/biotin activity was blocked using a commercially available blocking kit (Vector Laboratories, USA). Slides were incubated with primary antibodies detecting human Ki67 (DAKO M7240, USA, 1:350) and Cleaved Caspase-3 (Cell Signaling #9661, 1:100). Staining was visualized after incubation with biotinylated or peroxidase-bound secondary antibodies using streptavidin-biotin/horseradish peroxidase complex (Dako, USA, 1:100) and 3,3′-diaminobenzidine (Sigma-Aldrich, USA). Hematoxylin counterstaining was applied routinely, and hematoxylin & eosin (H&E) staining was used to analyze tissue viability and morphology. Photographs were acquired by digitalized scanning of slides using the NanoZoomer 2.0-HT multi-slide scanner (Hamamatsu, Japan). Ki67 stainings were quantified by scoring Ki67 positive nuclei in five randomly assigned 40× magnified areas from each slide. For Cleaved Caspase-3 stainings, the positive cytoplasm was scored with Aperia ImageScope software (Leica). Statistical significance was determined using one-way ANOVA with post-hoc Tukey's multiple comparison test.

2.9. Synergy determination

Drug synergy was assessed with the Chou-Talalay method in CompuSyn (Version 1.0, Combosyn incorporated) to determine the dose effect of combination therapy [27]. For this analysis, cells were treated with single inhibitors in increasing concentrations to determine a standard curve, and in combination using the IC_{20} of each compound. Strong synergism, synergism, additive effects and antagonism were defined by CI < 0.25, CI < 0.75, CI = 1 or CI > 1, respectively.

3. Results

3.1. mTORC1/2, PI3Kα/δ and MEK1/2 inhibitor susceptibility of OCCC cell lines

Considering the high mTORC1/2 inhibition susceptibility of OCCC [4], we searched for synergistic combinations with PI3K and MEK1/2 inhibitors. A panel of seven OCCC cell lines was selected, largely resembling the genetic makeup of OCCC, for evaluation of mTORC1/2, PI3K and MEK1/2 inhibitor sensitivity. We recently characterized PI3K/AKT/mTOR pathway and MAPK pathway alterations in these cell lines [4]. Alterations include activating hotspot mutations in the PI3K/AKT/mTOR pathway signaling node *PIK3CA*, deleterious mutations in *PTEN*, amplifications in *AKT1* and *AKT2* and a hotspot mutation in the MAPK pathway signaling node *KRAS* (Fig. 1A). Western blot analysis demonstrated universal expression of mTORC1/2 downstream target p-S6, indicating mTOR activity in all seven OCCC cell lines. Activity of PI3K (p-AKT^{308} and p-AKT^{473}) and MAPK (p-ERK) pathways, upstream of mTORC1/2, varied across the cell lines (Fig. 1B). We subsequently determined sensitivity towards mTORC1/2 inhibition (AZD8055), PI3Kα/δ inhibition (GDC0941) and MEK1/2 inhibition (selumetinib) using a short term (96 h) viability assay and defined cell line specific IC_{10}, IC_{20} and IC_{30} concentrations. All cell lines revealed nanomolar range AZD8055 sensitivity (Fig. 1C). GDC0941 and selumetinib sensitivity varied more widely across the cell lines (Fig. 1C). Gene alteration and protein phosphorylation status (Fig. 1A and B) did not correlate with sensitivity for these inhibitors (Mann-Whitney *U* test, data not shown), corresponding to an earlier report studying PI3K/AKT/mTOR inhibition in OCCC cell lines [28].

3.2. Synergistic effects of IC_{20} mTORC1/2, PI3Kα/δ and MEK1/2 inhibitor combinations

AZD8055, GDC0941 and selumetinib were combined at cell line specific IC_{20} concentrations calculated from short term viability assay results (Fig. 2A). IC_{10} and IC_{30} combinations were not further evaluated owing to high variation with the first and limited synergy due to the high efficacy of the latter with triple combinations. IC_{20} combinations of AZD8055 and GDC0941 induced synergistic effects (CI < 0.75) in two cell lines and the combination of AZD8055 with selumetinib in three cell lines (Fig. 2B, Supplementary Fig. 1A). Interestingly, the IC_{20} combination of AZD8055, GDC0941 and selumetinib (from here on

A

Cell line	Alteration						
	PIK3CA	*AKT1*	*AKT2*	*PIK3R1*	*PTEN*	*NRAS*	*BRAF*
ES2	wt	wt	wt	wt	wt	wt	V600E
HAC2	H1047R	wt	wt	wt	wt	wt	CNgain
JHOC5	wt	CNgain	CNgain	CNloss	wt	wt	wt
KOC7C	K111N	wt	wt	Q5R	233*, 323fs	wt	wt
RMG1	wt	CNgain	CNgain	wt	wt	wt	wt
SMOV2	H1047L	wt	CNgain	wt	wt	CNgain	wt
OVMANA	E545V	CNgain	CNgain	wt	wt	wt	wt

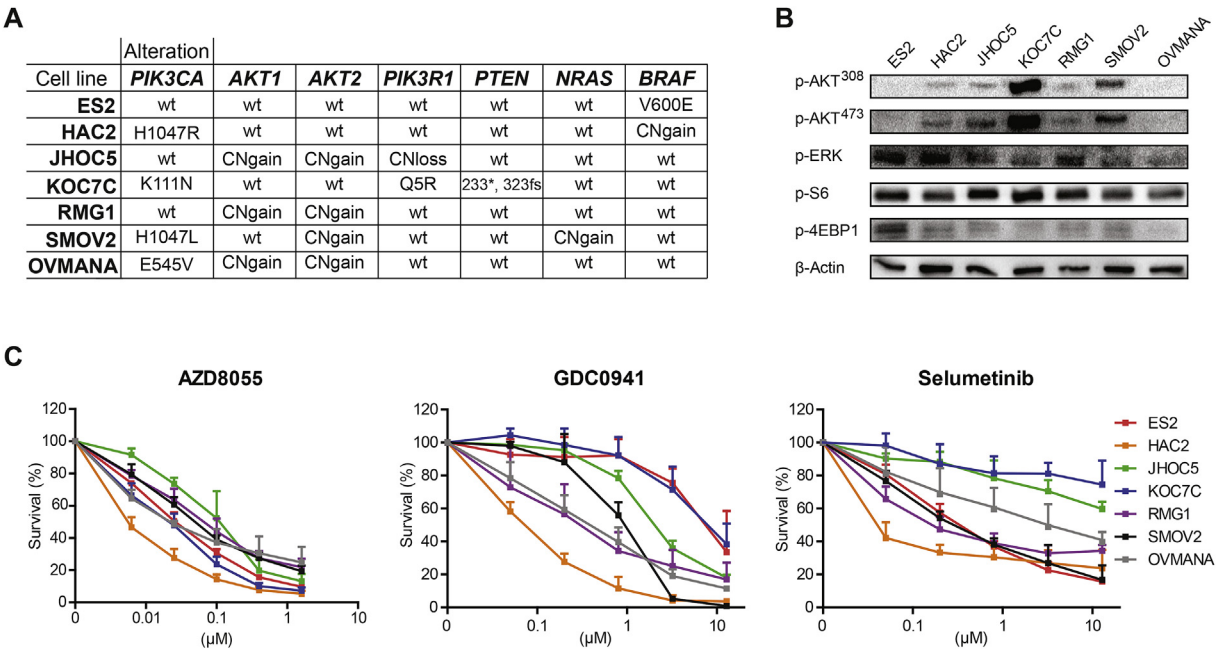

Fig. 1. Determination of monotherapy sensitivity in seven OCCC cell lines. (**A**) Mutations and CNAs in PI3K/AKT/mTOR pathway and MAPK pathway signaling nodes across seven OCCC cell lines [4]. wt indicates wild-type, CNgain indicates copy number gain, CNloss indicates copy number loss, * indicates stop-gained alteration, fs indicates frameshift alteration. (**B**) Expression of p-AKT^{308}, p-AKT^{473}, p-ERK, p-S6 and p-4EBP1 in the OCCC cell line panel determined by Western blot. β-Actin was used as loading control. (**C**) MTT assays with AZD8055, GDC0941 and selumetinib in the OCCC cell line panel. Error bars indicate SD and are derived from three experiments.

referred to as AGS), demonstrated strongly synergistic reduced survival (CI < 0.25) of JHOC5, KOC7C and RMG1 cells and synergistic survival reduction (CI < 0.75) of ES2 and SMOV2 cells. Only additive effects were observed in HAC2 and OVMANA cells, which might be related to their initial high sensitivity to all three inhibitors.

Single inhibitor IC_{20} treatment in long-term survival reduced growth in ES2 (GDC0941), HAC2 (AZD8055, GDC0941), JHOC5 (AZD8055, GDC0941), KOC7C (GDC0941) and OVMANA (selumetinib) (Fig. 2C). The combination of AZD8055 with either GDC0941 or selumetinib caused additional growth inhibition in SMOV2. Importantly, AGS induced a persistent growth reduction in all cell lines, confirming the results of the short term assays (Fig. 2C). MLN0128 (sapanisertib), another mTORC1/2 inhibitor currently in clinical development, reduced growth in combination with GDC0941 and selumetinib at IC_{20} concentrations as well (Supplementary Fig. 1B). The inhibitory effect of AGS was less profound in immortalized human retinal epithelial RPE1 cells, when treated with AGS at intermediate and high concentrations (Fig. 2C). At the molecular level, AZD8055 treatment led to upregulation of either p-ERK, p-AKT^{308} or p-AKT^{473} or combinations of these responses in HAC2, JHOC5, KOC7C, RMG1 and SMOV2 cells. Moreover, GDC0941 treatment induced p-ERK or p-AKT^{473} in three cell lines (JHOC5, KOC7C and RMG1), while selumetinib induced p-AKT^{473} in four cell lines (JHOC5, KOC7C, RMG1, and OVMANA) (Fig. 2D). These results indicate that combined treatment is essential to prevent single treatment induced pathway cross-activation. Interestingly, a near-universal reduction of p-AKT^{308}, p-AKT^{473}, and p-ERK was observed with AGS resulting in a downstream reduction of p-S6 and p-4EBP1, another transcriptional regulator downstream of mTORC1 [29], across all our OCCC cell lines (Fig. 2D). MLN0128 in combination with GDC0941 and selumetinib demonstrated similar results (Supplementary Fig. 1C).

In conclusion, synergistic growth inhibition was observed with AGS in five OCCC cell lines and an additive effect with AGS in two other OCCC cell lines. This observation was supported by long-term survival assays and extensive downregulation of phosphorylated target proteins of the PI3K/AKT/mTOR pathway and MAPK pathway.

3.3. Low-dose mTORC1/2, PI3Kα/δ and MEK1/2 inhibitor combination is effective in OCCC PDX models

Next, we explored the effect of combining AZD8055, GDC0941 and selumetinib at low-dose in vivo in an unbiased manner by using two unique OCCC PDX models. Both PDX.180 and PDX.247 tumors have PI3K/AKT/mTOR pathway related alterations (Fig. 3A). To mimic the IC_{20} concentrations used in vitro, dosing for each drug was set at 20% of the maximum dose daily used for monotherapy in mice, as described [30–32]. Growth inhibition was observed in AZD8055, GDC0941 and selumetinib single treatment arms as compared to vehicle. The effect of monotherapy treatment became significant at day 21 in both PDX models (Supplementary Fig. 2A). AGS low-dose combination treatment caused significant tumor regression in PDX.180 and significantly reduced tumor growth in PDX.247 bearing mice (Fig. 3B and C). Importantly, weight of the mice remained stable during the course of treatment and none of the mice had to be prematurely sacrificed suggesting no combination treatment related systemic toxicity (Fig. 3D and E). Reduced expression of the proliferation marker Ki67 and an increase in apoptosis (active Caspase-3) accompanied tumor regression in PDX.180 mice in the AGS low-dose combination treatment arm (Fig. 4A and B). Reduced Ki67 expression was also observed in the AGS low-dose combination treatment arm of PDX.247 mice (Fig. 4C and D). The inhibitory effect of the combination treatment was stronger than that of 10 mg/kg AZD8055 treatment in PDX.180 mice in historical data [4]. A similar growth reduction was observed with the combination treatment and 10 mg/kg AZD8055 in PDX.247 mice (Supplementary Figs. 2A–B) [4].

3.4. The Bcl-2, Bcl-XL and Bcl-w inhibitor ABT-737 enhances efficacy of AGS in OCCC cells

AGS had a strong effect on growth of OCCC cells in both short term and long term assays. However, no apoptosis was induced by AGS treatment and regrowth of OCCC cell lines was observed after AGS was removed from the media (data not shown). Remarkably, the AGS low-

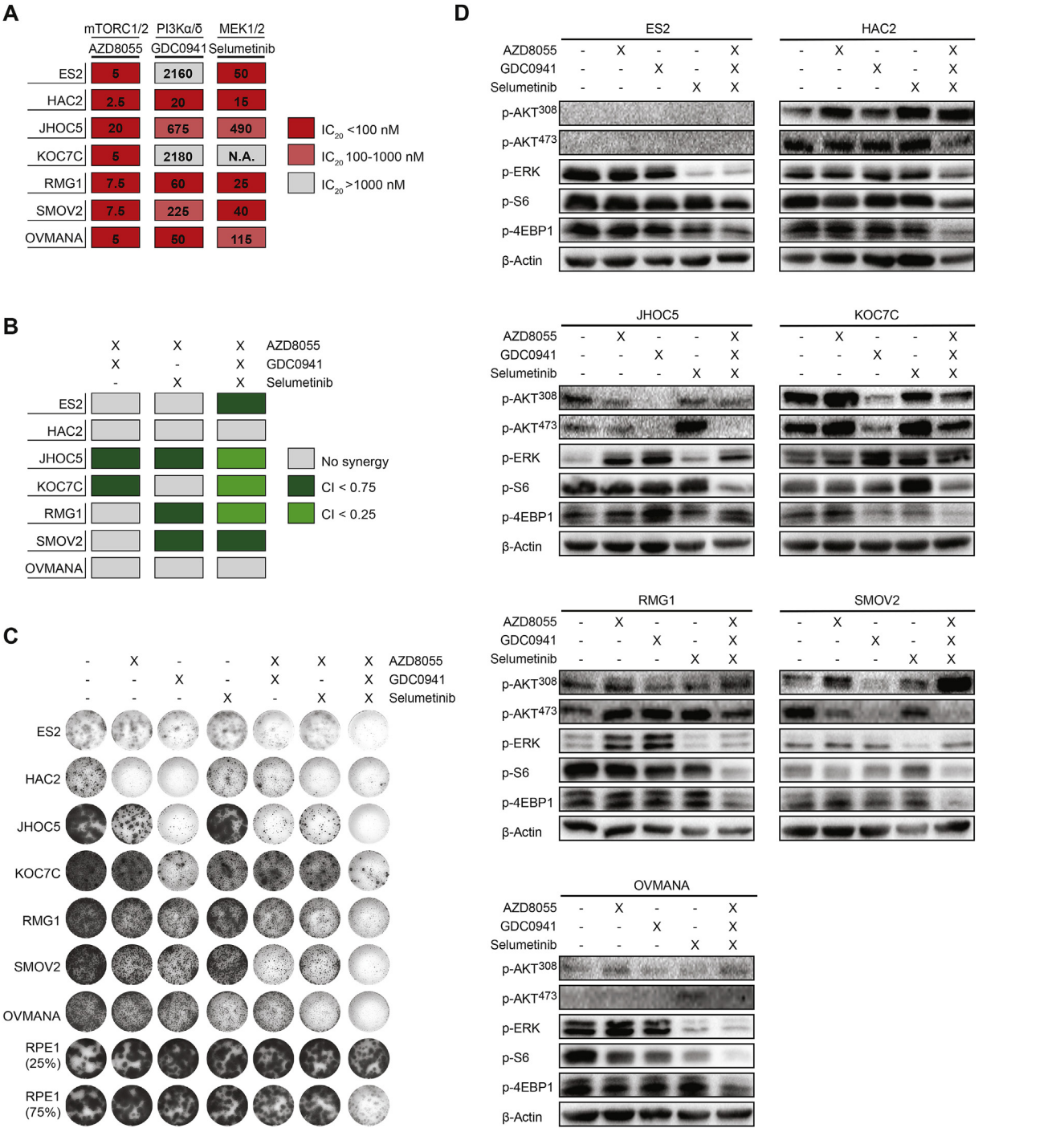

Fig. 2. Synergystic IC_{20} combination effects of AZD8055, GDC0941 and selumetinib. (**A**) IC_{20} concentrations as determined from MTT assay data. KOC7C IC_{20} for selumetinib could not be determined within the used concentration range. Accordingly, KOC7C was treated with 5 μM selumetinib in subsequent experiments. (**B**) Synergy determination of AZD8055, GDC0941 and selumetinib IC_{20} combinations in the OCCC cell line panel with the Talalay–Chou method [27]. Combinations were regarded synergistic when Combination Index (CI) < 0.75 or < 0.25 was observed in at least two out of three MTT assay experiments. (**C**) AGS inhibitory effects were measured in a long-term colony formation assay. RPE1 cells were treated with 25% (5 nM AZD8055, 540 nM GDC0941 and 119 nM selumetinib) and 75% (15 nM AZD8055, 1620 nM GDC0941 and 356 nM selumetinib) of the difference between the lowest and highest IC_{20} from our OCCC cell line panel. Results shown are representative of two experiments (**D**) Expression of p-AKT^{308}, p-AKT^{473}, p-ERK, p-S6 and p-4EBP1 after 48 h of treatment with IC_{20} concentration of AZD8055, GDC0941, selumetinib or AGS as determined by Western blot. β-Actin was used as loading control. Membranes were individually exposed to visualize protein bands. Results shown are representative of three experiments.

dose combination did induce apoptosis in PDX.180 but not in the second model (PDX.247). These results suggest that apoptosis induction may contribute to the efficacy of the AGS combination in vivo. Therefore, we investigated whether AGS in combination with cisplatin would affect proliferation and apoptosis in OCCC cell lines, since platinum-based chemotherapy is still the standard of care for OCCC patients, despite its limited efficacy in this *TP53* wild-type ovarian cancer subtype [4,33,34]. Cisplatin did not induce massive apoptosis in OCCC cell lines, also not at high doses (Supplementary Fig. 3A and results not shown). Disappointingly, AGS did not enhance proliferation

A

Alteration	*PIK3CA*	*AKT2*	*PIK3R2*
PDX.180	K111E	CNgain	CNgain
PDX.247	wt	CNgain	wt

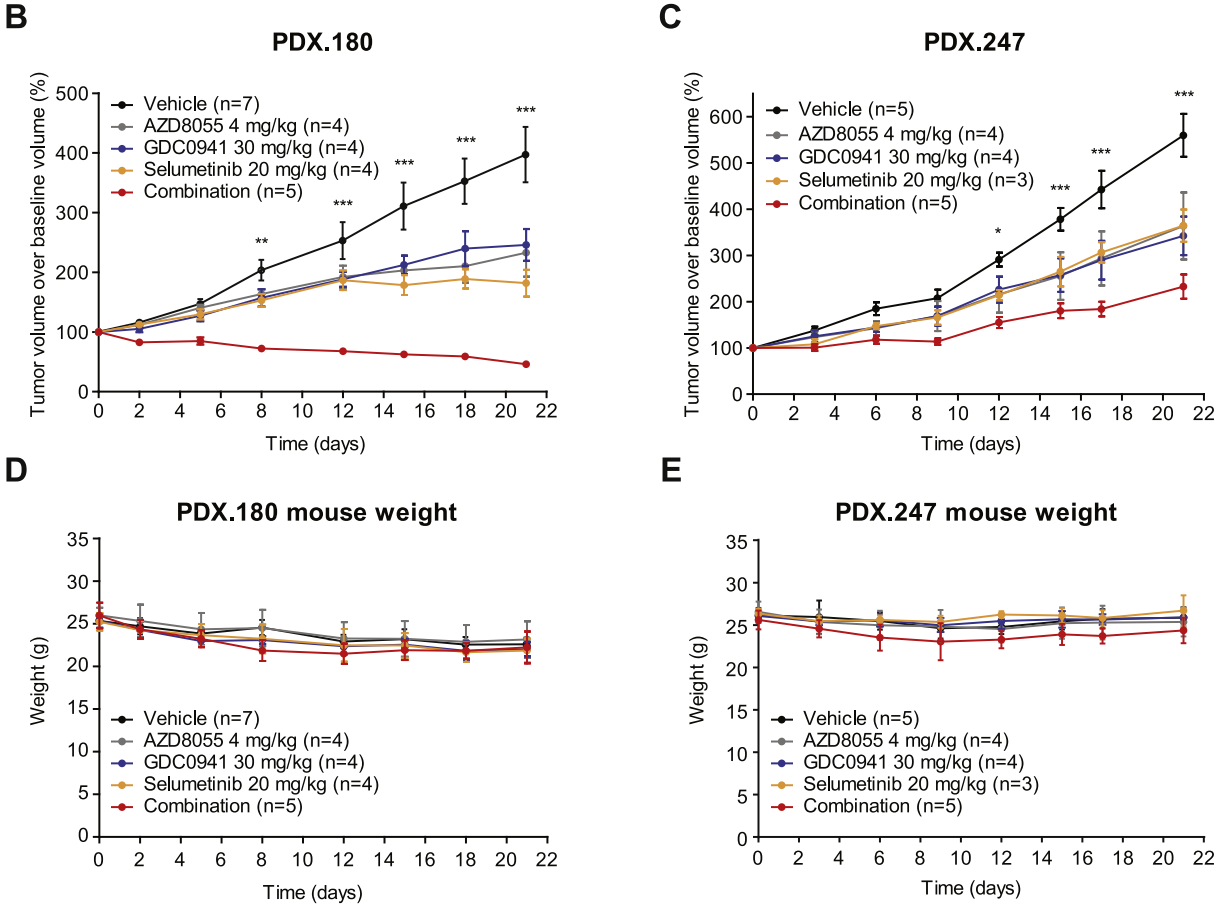

Fig. 3. Low-dose AZD8055, GDC0941 and selumetinib combination efficacy in OCCC PDX models. (**A**) Mutations and CNAs in PI3K/AKT/mTOR signaling nodes in PDX.180 and PDX.247 [4]. PDX.180 (**B**) and PDX.247 (**C**) NSG mice treated with vehicle, AZD8055, GDC0941, selumetinib or the combination in F5 generation. Tumor volume is represented as percentage of initial tumor volume at start of treatment. In the PDX.180 vehicle arm three mice received oral gavage vehicle treatment. Four mice received intraperitoneal vehicle treatment and are previously described by Caumanns et al. [4]. Error bars indicate SEM, * indicates $p < 0.05$, ** indicates $p < 0.01$ and *** indicates $p < 0.001$ of combination treatment arm relative to vehicle treatment arm. PDX.180 (**D**) and PDX.247 (**E**) mouse weight represented for the aforementioned treatment groups. Error bars indicate SD.

inhibition and apoptosis induction by cisplatin, suggesting that the mechanisms through which AGS and cisplatin act do not beneficially interact in OCCC (Supplementary Figs. 3A–B). These results led us to further investigate whether a specific apoptosis inducing agent could sensitize OCCC cells towards AGS. To this end, the efficacy of ABT-737, an inhibitor of the anti-apoptotic proteins Bcl-2, Bcl-X_L and Bcl-w [35], was evaluated in our cell line panel. ABT-737 treatment inhibited proliferation and this effect was additive to the effect of AGS treatment on proliferation of all cell lines, with ES2 being the exception (Fig. 5A). The combination of AGS and ABT-737 significantly enhanced apoptosis compared to both AGS and ABT-737 single treatment in HAC2, KOC7C, and SMOV2 cells (Fig. 5B and C and Supplementary Fig. 3C). This observation was supported by an increase in the apoptotic markers active PARP or active Caspase-3 in KOC7C and SMOV2 cells. In OV-MANA cells the combination effect was less clear reflecting the different levels of sensitivity to the combination (Fig. 5D).

4. Discussion

New therapeutic strategies for the treatment of OCCC are urgently needed because of the low efficacy of standard platinum-based chemotherapy in advanced stage OCCC. Here, we demonstrate synergistic effects of mTORC1/2 (AZD8055), PI3K (GDC0941) and MEK1/2 (selumetinib) inhibitors combined at low-dose in a genetically diverse panel of OCCC cell lines and OCCC PDX models. Our study signifies that combining mTORC1/2, PI3K and MEK1/2 inhibitors at low-dose is an effective treatment strategy that precludes low-dose single treatment induced pathway rewiring and warrants further exploration in OCCC.

In our recent report, we demonstrated high susceptibility of OCCC to mTORC1/2 inhibitors, however, we also observed PI3K/AKT/mTOR pathway re-activation [4]. Therefore, we evaluated whether PI3K and MEK1/2 inhibitors can add to the potency of mTORC1/2 inhibitors to prevent pathway re-activation and cross-activation at suboptimal concentrations. Indeed, IC_{20} combinations of AZD8055, GDC0941 and selumetinib (AGS) decreased single-inhibitor related re-activation of PI3K/AKT/mTOR and MAPK pathways at the molecular level. Our in vitro results of the AGS combination indicate that the efficacy of AGS covers the mutational spectra found in PI3K/AKT/mTOR pathway and MAPK pathway nodes in OCCC. Moreover, the well tolerated low-dose AGS combination efficiently reduced tumor growth in two OCCC PDX

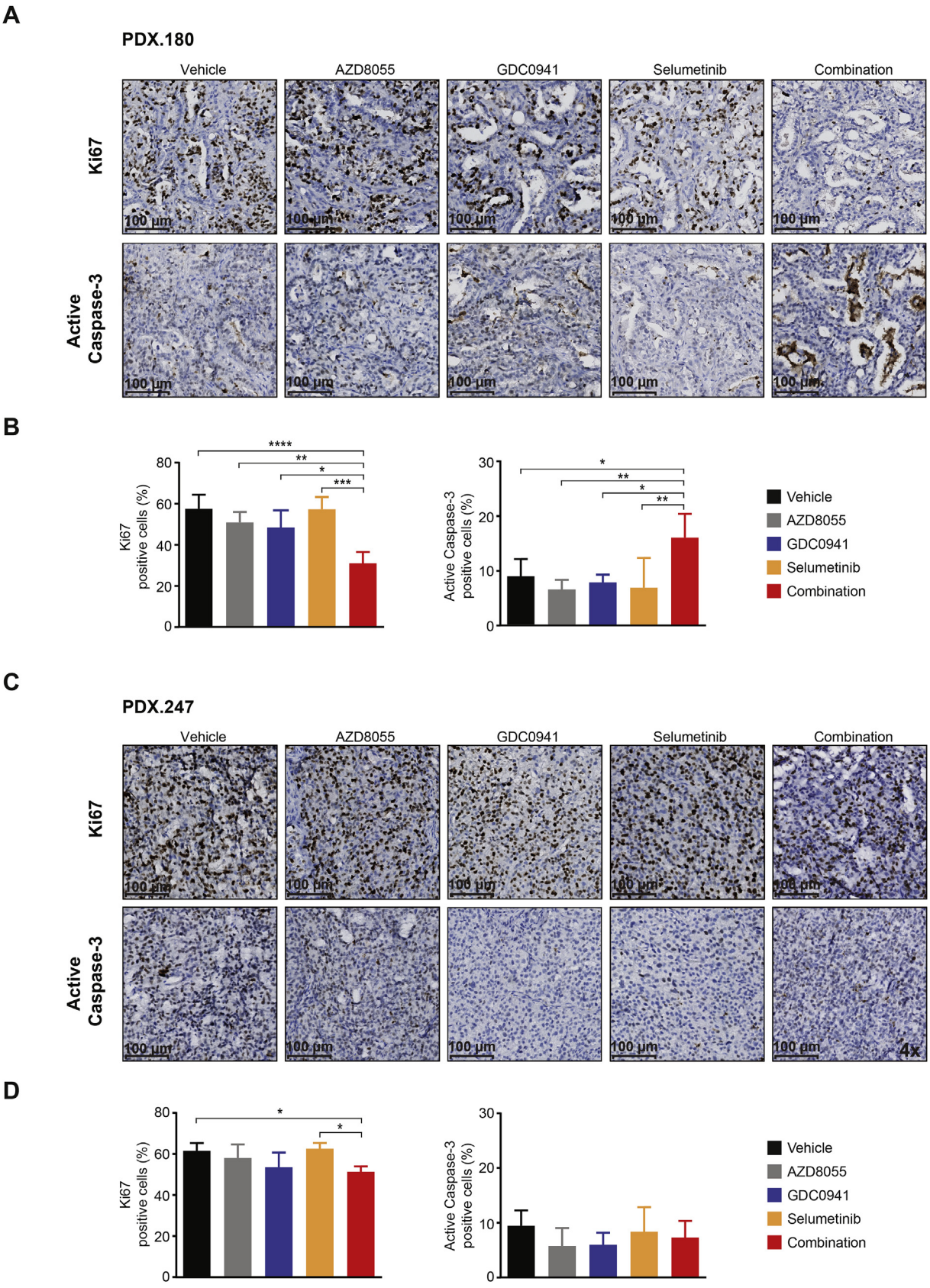

Fig. 4. Ki67 and active Caspase-3 expression in OCCC PDX models. Representative expression and quantification of Ki67 and active (cleaved) Caspase-3 in the vehicle, AZD8055, GDC0941, selumetinib or combination treatment groups in PDX.180 (**A** and **B**) and PDX.247 (**C** and **D**) as determined by IHC. Error bars indicate SD. * indicates $p < 0.05$, ** indicates $p < 0.01$ and *** indicates $p < 0.001$.

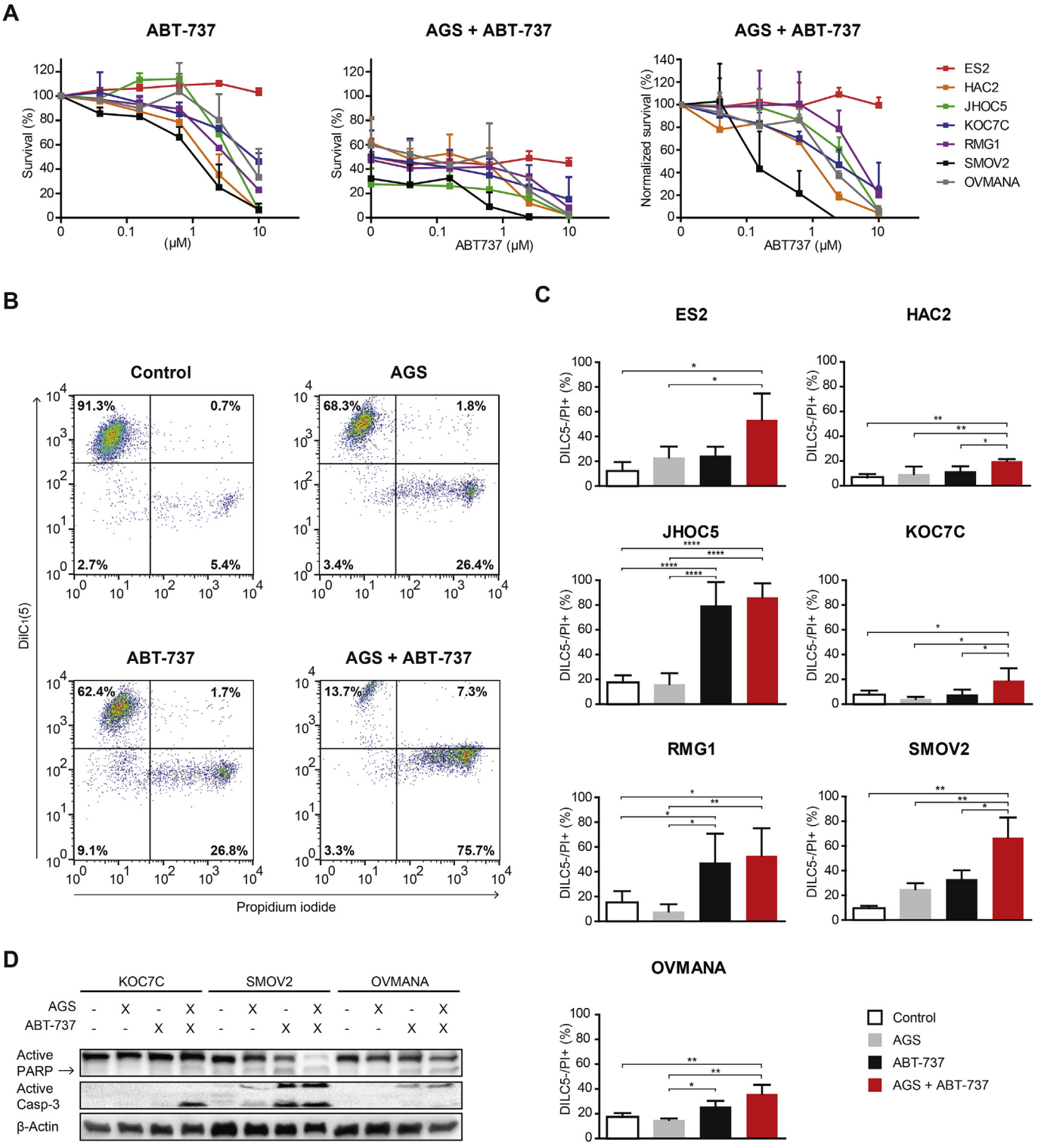

Fig. 5. ABT-737 added to IC_{20} AZD8055, GDC0941 and selumetinib combination. (**A**) Sensitivity of ABT-737, ABT-737 with AGS (and normalized to AGS) as determined by MTT assay. Error bars indicate SD and are derived from two experiments. Flow cytometry plots from $DiIC_1$ (5)-PI flow cytometry analysis of SMOV2 (**B**) after 48 h treatment with AGS, 1 μM ABT-737 or the combination. (**C**) Quantification of the bottom two quadrants ($DiIC_1$ (5)-/PI- and $DiIC_1$ (5)-/PI+) from $DiIC_1$ (5)-PI flow cytometry analysis after 48 h treatment with AGS, ABT-737 or the combination in the cell line panel. HAC2, SMOV2 and OVMANA were treated with 1 μM ABT-737. ES2, JHOC5, KOC7C and RMG1 were treated with 10 μM ABT-737. Error bars indicate SD and are derived from three experiments. * indicates $p < 0.05$, ** indicates $p < 0.01$, *** indicates $p < 0.001$ and **** indicates $p < 0.0001$. (**D**) Expression of active (cleaved) PARP and active (cleaved) Caspase-3 after 48 h of treatment with AGS, 1 μM ABT-737 or 1 μM ABT-737 added to AGS as determined by Western blot. Floating cells were included in lysate. β-Actin was used as loading control. Results shown are representative of two experiments.

models, which we have recently established and are more accurately representing patient tumors than cell line based xenografts [4,26,36].

Considering that single-targeted kinase inhibition results in kinome rewiring and resistance in various tumor models, more cancers are expected to benefit from combined inhibition of mTORC1/2, PI3K and MEK1/2 [37,38]. Synergistic combinations of PI3K-mTORC1/2 inhibition and MEK1/2 inhibition have indeed been successfully used preclinically in multiple cancer types (serous and mucinous ovarian cancer, endometrial cancer and melanoma) with PI3K/AKT/mTOR pathway and MAPK pathway alterations [39–42]. Moreover, single long-dose treatment might result in more resistant clonal tumor cells [43,44], which can be prevented by combination treatment. Notably, autophagy was shown to play an important role in cisplatin resistance in OCCC cells [45]. In addition, single-targeted inhibition by AZD8055 in colon cells antagonized chemotherapy initiated cell death through autophagy induction [46]. These findings might explain why cisplatin added to AGS was not effective in our study. Taken together, these results suggest that OCCC patients potentially benefit from a combination of mTORC1/2, PI3K and MEK1/2 inhibitors using low-doses and that this strategy could be extrapolated to other cancer types.

The in vitro and in vivo results demonstrated growth inhibition for all models that often not coincided with apoptosis induction, suggesting additional treatment options are needed. We observed that exposure of OCCC cell lines to the apoptosis inducing agent ABT-737 increased responsiveness towards AGS. These results are in line with previous work in serous ovarian cancer cell lines and PDX models combining dual PI3K-mTORC1/2 or MEK1/2 inhibitors with ABT-737 or navitoclax (ABT-263) [47–49]. Interestingly, the low-dose AGS combination induced apoptosis in our most sensitive OCCC PDX model, suggesting that apoptosis enhancers may not always be necessary for apoptosis induction. Recently, we found that BET-bromodomain inhibitors have synthetic lethal effects in *ARID1A* mutant OCCC [6]. BET-bromodomain inhibitors have been shown to reduce kinase inhibition related pathway rewiring and re-activation in multiple cancer models, including *ARID1A* mutant ovarian cancer cells [37,38]. Therefore, the combination of AGS with BET-bromodomain inhibitors may be especially of interest in the context of *ARID1A* mutant OCCC. Alternatively, given the high alteration frequency in DNA repair pathway genes in OCCC [4,9], combining DNA damaging agents or DNA repair pathway inhibitors with either AGS or mTORC1/2, PI3K, and MEK1/2 inhibitors individually could be an attractive approach for future studies. This will require careful titration of drug combinations to increase treatment efficacy by modulating autophagy and apoptosis induction in OCCC.

PI3K-mTORC1/2 dual inhibitor and MEK1/2 inhibitor combinations have been explored clinically. The PI3K-mTORC1/2 dual inhibitor gedatolisib showed preliminary antitumor efficacy in a subset of *KRAS* mutant ovarian cancer patients when combined with PD-0325901. Unfortunately, adverse event related treatment interruptions (mainly gastrointestinal complications) and dose-limiting toxicity occurred in over half of the patients. Notably, the treatment arm combining the other PI3K-mTORC1/2 inhibitor PF-04691502 with PD-0325901 was prematurely closed due to low tolerability [50]. Dose-limiting toxicity or treatment discontinuation occurred in other combination trials with PI3K-mTORC1/2 dual inhibitors and MEK inhibitors as well, which included ovarian cancer (NCT01936363 and NCT01248858) [51–53]. Importantly, stable disease or partial responses were observed in some patients from distinct cancer types, indicating that combined inhibition of mTORC1/2, PI3K and MEK1/2 may have therapeutic benefit. These clinical results advocate the use of separate inhibitors of mTORC1/2 and PI3K to prevent target related toxicity as observed with PI3K-mTORC1/2 dual inhibitors. Moreover, to safely add a MEK1/2 inhibitor to mTORC1/2 and PI3K inhibitor combinations careful titration of such a putative low-dose triple combination will be crucial. Titrated low-dose combinations of targeted drugs have already been used in cancer patients and efficacy was observed with minimal dose-limiting toxicity [54–56]. For this low-dose strategy, multiple inhibitors of mTORC1/2, PI3K or MEK1/2, currently in phase II trials (NCT01737450, NCT02101788, NCT02465060, NCT02725268, NCT03128619 and NCT03264066), are available.

Collectively, the effectiveness of low-dose mTORC1/2, PI3K and MEK1/2 inhibitor combinations in OCCC cell lines and PDX models signifies exploration of this low-dose treatment strategy in future clinical trials in OCCC and other cancer types with PI3K/AKT/mTOR and MAPK pathway alterations.

Ethics approval and consent to participate

This study was performed in accordance with the declaration of Helsinki. Before surgery, all patients from whom tumor samples were obtained for PDX modeling gave written informed consent.

Availability of data and materials

All data generated or analyzed during this study are included in this published article.

Conflicts of interest

The authors declare no potential conflicts of interest.

Funding

This research was supported by grants from the Dutch Cancer Society (KWF, RUG 2012-5477) and the Cock-Hadders foundation.

Author contributions

A.G.J.Z., G.B.A.W. and S.J. conceived and supervised the project. J.J.C. and A.W. performed the majority of experiments and data analysis with the assistance of G.J.M. and A.K. J.J.C., A.G.J.Z., G.B.A.W. and S.J. wrote the manuscript with the assistance of M.J. and R.B. All authors discussed the results and commented on the manuscript.

Acknowledgements

We acknowledge Dr. Hiroaki Itamochi and Dr. Els Berns for their kind contribution of OCCC cell lines. The authors thank Gerda de Vries and Fernanda X. Rosas Plaza for help with the PDX models. G. Bea A. Wisman and Steven de Jong are members of the EurOPDX Consortium.

Appendix A. Supplementary data

Supplementary data to this article can be found online at https://doi.org/10.1016/j.canlet.2019.07.004.

References

[1] K.E. Oliver, W.E. Brady, M. Birrer, D.M. Gershenson, G. Fleming, L.J. Copeland, et al., An evaluation of progression free survival and overall survival of ovarian cancer patients with clear cell carcinoma versus serous carcinoma treated with platinum therapy: an NRG Oncology/Gynecologic Oncology Group experience, Gynecol. Oncol. 147 (2) (2017 Nov) 243–249.

[2] K.C. Wiegand, S.P. Shah, O.M. Al-Agha, Y. Zhao, K. Tse, T. Zeng, et al., ARID1A mutations in endometriosis-associated ovarian carcinomas, N. Engl. J. Med. 363 (16) (2010 Oct 14) 1532–1543.

[3] S. Jones, T.L. Wang, I. Shih, T.L. Mao, K. Nakayama, R. Roden, et al., Frequent mutations of chromatin remodeling gene ARID1A in ovarian clear cell carcinoma, Science 330 (6001) (2010 Oct 8) 228–231.

[4] J.J. Caumanns, K. Berns, G.B.A. Wisman, R.S.N. Fehrmann, T. Tomar, H. Klip, et al., Integrative kinome profiling identifies mTORC1/2 inhibition as treatment strategy in ovarian clear cell carcinoma, Clin. Cancer Res. 24 (16) (2018 Aug 15) 3928–3940.

[5] B.G. Bitler, K.M. Aird, A. Garipov, H. Li, M. Amatangelo, A.V. Kossenkov, et al., Synthetic lethality by targeting EZH2 methyltransferase activity in ARID1A-mutated cancers, Nat. Med. 21 (3) (2015 Mar) 231–238.

[6] K. Berns, J.J. Caumanns, E.M. Hijmans, A.M.C. Gennissen, T.M. Severson, B. Evers, et al., ARID1A mutation sensitizes most ovarian clear cell carcinomas to BET

inhibitors, Oncogene 37 (33) (2018 Aug) 4611–4625.
[7] K.T. Kuo, T.L. Mao, S. Jones, E. Veras, A. Ayhan, T.L. Wang, et al., Frequent activating mutations of PIK3CA in ovarian clear cell carcinoma, Am. J. Pathol. 174 (5) (2009 May) 1597–1601.
[8] Y. Hashiguchi, H. Tsuda, T. Inoue, R.S. Berkowitz, S.C. Mok, PTEN expression in clear cell adenocarcinoma of the ovary, Gynecol. Oncol. 101 (1) (2006 Apr) 71–75.
[9] M.L. Friedlander, K. Russell, S. Millis, Z. Gatalica, R. Bender, A. Voss, Molecular profiling of clear cell ovarian cancers: identifying potential treatment targets for clinical trials, Int. J. Gynecol. Cancer 26 (4) (2016 May) 648–654.
[10] H. Itamochi, T. Oishi, N. Oumi, S. Takeuchi, K. Yoshihara, M. Mikami, et al., Whole-genome sequencing revealed novel prognostic biomarkers and promising targets for therapy of ovarian clear cell carcinoma, Br. J. Canc. 117 (5) (2017 Aug 22) 717–724.
[11] R. Murakami, N. Matsumura, J.B. Brown, K. Higasa, T. Tsutsumi, M. Kamada, et al., Exome sequencing landscape analysis in ovarian clear cell carcinoma shed light on key chromosomal regions and mutation gene networks, Am. J. Pathol. 187 (10) (2017 Oct) 2246–2258.
[12] G.F. Zannoni, G. Improta, G. Chiarello, A. Pettinato, M. Petrillo, P. Scollo, et al., Mutational status of KRAS, NRAS, and BRAF in primary clear cell ovarian carcinoma, Virchows Arch. 465 (2) (2014 Aug) 193–198.
[13] D.S. Tan, M. Iravani, W.G. McCluggage, M.B. Lambros, F. Milanezi, A. Mackay, et al., Genomic analysis reveals the molecular heterogeneity of ovarian clear cell carcinomas, Clin. Cancer Res. 17 (6) (2011 Mar 15) 1521–1534.
[14] A. Okamoto, J. Sehouli, N. Yanaihara, Y. Hirata, I. Braicu, B.G. Kim, et al., Somatic copy number alterations associated with Japanese or endometriosis in ovarian clear cell adenocarcinoma, PLoS One 10 (2) (2015 Feb 6) e0116977.
[15] E.M. Posadas, M.S. Liel, V. Kwitkowski, L. Minasian, A.K. Godwin, M.M. Hussain, et al., A phase II and pharmacodynamic study of gefitinib in patients with refractory or recurrent epithelial ovarian cancer, Cancer 109 (7) (2007 Apr 1) 1323–1330.
[16] S.V. Blank, P. Christos, J.P. Curtin, N. Goldman, C.D. Runowicz, J.A. Sparano, et al., Erlotinib added to carboplatin and paclitaxel as first-line treatment of ovarian cancer: a phase II study based on surgical reassessment, Gynecol. Oncol. 119 (3) (2010 Dec) 451–456.
[17] A.A. Garcia, M.W. Sill, H.A. Lankes, A.K. Godwin, R.S. Mannel, D.K. Armstrong, et al., A phase II evaluation of lapatinib in the treatment of persistent or recurrent epithelial ovarian or primary peritoneal carcinoma: a gynecologic oncology group study, Gynecol. Oncol. 124 (3) (2012 Mar) 569–574.
[18] Y. Shi, H. Yan, P. Frost, J. Gera, A. Lichtenstein, Mammalian target of rapamycin inhibitors activate the AKT kinase in multiple myeloma cells by up-regulating the insulin-like growth factor receptor/insulin receptor substrate-1/phosphatidylinositol 3-kinase cascade, Mol. Cancer Ther. 4 (10) (2005 Oct) 1533–1540.
[19] K.E. O'Reilly, F. Rojo, Q.B. She, D. Solit, G.B. Mills, D. Smith, et al., mTOR inhibition induces upstream receptor tyrosine kinase signaling and activates Akt, Cancer Res. 66 (3) (2006 Feb 1) 1500–1508.
[20] E. Rozengurt, H.P. Soares, J. Sinnet-Smith, Suppression of feedback loops mediated by PI3K/mTOR induces multiple overactivation of compensatory pathways: an unintended consequence leading to drug resistance, Mol. Cancer Ther. 13 (11) (2014 Nov) 2477–2488.
[21] T. Oishi, H. Itamochi, A. Kudoh, M. Nonaka, M. Kato, M. Nishimura, et al., The PI3K/mTOR dual inhibitor NVP-BEZ235 reduces the growth of ovarian clear cell carcinoma, Oncol. Rep. 32 (2) (2014 Aug) 553–558.
[22] P. Yu, A.D. Laird, X. Du, J. Wu, K.A. Won, K. Yamaguchi, et al., Characterization of the activity of the PI3K/mTOR inhibitor XL765 (SAR245409) in tumor models with diverse genetic alterations affecting the PI3K pathway, Mol. Cancer Ther. 13 (5) (2014 May) 1078–1091.
[23] N. Fazio, R. Buzzoni, E. Baudin, L. Antonuzzo, R.A. Hubner, H. Lahner, et al., A phase II study of BEZ235 in patients with everolimus-resistant, advanced pancreatic neuroendocrine tumours, Anticancer Res. 36 (2) (2016 Feb) 713–719.
[24] K.P. Papadopoulos, J. Tabernero, B. Markman, A. Patnaik, A.W. Tolcher, J. Baselga, et al., Phase I safety, pharmacokinetic, and pharmacodynamic study of SAR245409 (XL765), a novel, orally administered PI3K/mTOR inhibitor in patients with advanced solid tumors, Clin. Cancer Res. 20 (9) (2014 May 1) 2445–2456.
[25] T.F. Meehan, N. Conte, T. Goldstein, G. Inghirami, M.A. Murakami, S. Brabetz, et al., PDX-MI: minimal information for patient-derived tumor xenograft models, Cancer Res. 77 (21) (2017 Nov 1) e62–e66.
[26] N.G. Alkema, T. Tomar, E.W. Duiker, G. Jan Meersma, H. Klip, A.G. van der Zee, et al., Biobanking of patient and patient-derived xenograft ovarian tumour tissue: efficient preservation with low and high fetal calf serum based methods, Sci. Rep. 5 (2015 Oct 6) 14495.
[27] T.C. Chou, Drug combination studies and their synergy quantification using the Chou-Talalay method, Cancer Res. 70 (2) (2010 Jan 15) 440–446.
[28] M. Rahman, K. Nakayama, M.T. Rahman, N. Nakayama, M. Ishikawa, A. Katagiri, et al., Clinicopathologic and biological analysis of PIK3CA mutation in ovarian clear cell carcinoma, Hum. Pathol. 43 (12) (2012 Dec) 2197–2206.
[29] Q.B. She, E. Halilovic, Q. Ye, W. Zhen, S. Shirasawa, T. Sasazuki, et al., 4E-BP1 is a key effector of the oncogenic activation of the AKT and ERK signaling pathways that integrates their function in tumors, Cancer Cell 18 (1) (2010 Jul 13) 39–51.
[30] J. Renshaw, K.R. Taylor, R. Bishop, M. Valenti, A. De Haven Brandon, S. Gowan, et al., Dual blockade of the PI3K/AKT/mTOR (AZD8055) and RAS/MEK/ERK (AZD6244) pathways synergistically inhibits rhabdomyosarcoma cell growth in vitro and in vivo, Clin. Cancer Res. 19 (21) (2013 Nov 1) 5940–5951.
[31] F.I. Raynaud, S.A. Eccles, S. Patel, S. Alix, G. Box, I. Chuckowree, et al., Biological properties of potent inhibitors of class I phosphatidylinositide 3-kinases: from PI-103 through PI-540, PI-620 to the oral agent GDC-0941, Mol. Cancer Ther. 8 (7) (2009 Jul) 1725–1738.
[32] T.C. Yeh, V. Marsh, B.A. Bernat, J. Ballard, H. Colwell, R.J. Evans, et al., Biological characterization of ARRY-142886 (AZD6244), a potent, highly selective mitogen-activated protein kinase kinase 1/2 inhibitor, Clin. Cancer Res. 13 (5) (2007 Mar 1) 1576–1583.
[33] D.S. Tan, R.E. Miller, S.B. Kaye, New perspectives on molecular targeted therapy in ovarian clear cell carcinoma, Br. J. Canc. 108 (8) (2013 Apr 30) 1553–1559.
[34] Y.K. Wang, A. Bashashati, M.S. Anglesio, D.R. Cochrane, D.S. Grewal, G. Ha, et al., Genomic consequences of aberrant DNA repair mechanisms stratify ovarian cancer histotypes, Nat. Genet. 49 (6) (2017 Jun) 856–865.
[35] T. Oltersdorf, S.W. Elmore, A.R. Shoemaker, R.C. Armstrong, D.J. Augeri, B.A. Belli, et al., An inhibitor of Bcl-2 family proteins induces regression of solid tumours, Nature 435 (7042) (2005 Jun 2) 677–681.
[36] M. Hidalgo, F. Amant, A.V. Biankin, E. Budinska, A.T. Byrne, C. Caldas, et al., Patient-derived xenograft models: an emerging platform for translational cancer research, Cancer Discov. 4 (9) (2014 Sep) 998–1013.
[37] T.J. Stuhlmiller, S.M. Miller, J.S. Zawistowski, K. Nakamura, A.S. Beltran, J.S. Duncan, et al., Inhibition of lapatinib-induced kinome reprogramming in ERBB2-positive breast cancer by targeting BET family bromodomains, Cell Rep. 11 (3) (2015 Apr 21) 390–404.
[38] E.E. Stratikopoulos, M. Dendy, M. Szabolcs, A.J. Khaykin, C. Lefebvre, M.M. Zhou, et al., Kinase and BET inhibitors together clamp inhibition of PI3K signaling and overcome resistance to therapy, Cancer Cell 27 (6) (2015 Jun 8) 837–851.
[39] K.E. Sheppard, C. Cullinane, K.M. Hannan, M. Wall, J. Chan, F. Barber, et al., Synergistic inhibition of ovarian cancer cell growth by combining selective PI3K/mTOR and RAS/ERK pathway inhibitors, Eur. J. Cancer 49 (18) (2013 Dec) 3936–3944.
[40] K. Inaba, K. Oda, K. Aoki, K. Sone, Y. Ikeda, A. Miyasaka, et al., Synergistic anti-tumor effects of combination PI3K/mTOR and MEK inhibition (SAR245409 and pimasertib) in mucinous ovarian carcinoma cells by fluorescence resonance energy transfer imaging, Oncotarget 7 (20) (2016 May 17) 29577–29591.
[41] K. Inaba, K. Oda, Y. Ikeda, K. Sone, A. Miyasaka, T. Kashiyama, et al., Antitumor activity of a combination of dual PI3K/mTOR inhibitor SAR245409 and selective MEK1/2 inhibitor pimasertib in endometrial carcinomas, Gynecol. Oncol. 138 (2) (2015 Aug) 323–331.
[42] C. Posch, H. Moslehi, L. Feeney, G.A. Green, A. Ebaee, V. Feichtenschlager, et al., Combined targeting of MEK and PI3K/mTOR effector pathways is necessary to effectively inhibit NRAS mutant melanoma in vitro and in vivo, Proc. Natl. Acad. Sci. U. S. A. 110 (10) (2013 Mar 5) 4015–4020.
[43] N. Hagiwara, M. Watanabe, M. Iizuka-Ohashi, I. Yokota, S. Toriyama, M. Sukeno, et al., Mevalonate pathway blockage enhances the efficacy of mTOR inhibitors with the activation of retinoblastoma protein in renal cell carcinoma, Cancer Lett. 431 (2018 Sep 1) 182–189.
[44] X. Dai, H. Xia, S. Zhou, Q. Tang, F. Bi, Zoledronic acid enhances the efficacy of the MEK inhibitor trametinib in KRAS mutant cancers, Cancer Lett. 442 (2019 Feb 1) 202–212.
[45] K.K. Chan, O.G. Wong, E.S. Wong, K.K. Chan, P.P. Ip, K.Y. Tse, et al., Impact of iASPP on chemoresistance through PLK1 and autophagy in ovarian clear cell carcinoma, Int. J. Cancer 143 (6) (2018 Sep 15) 1456–1469.
[46] S. Huang, Z.J. Yang, C. Yu, F.A. Sinicrope, Inhibition of mTOR kinase by AZD8055 can antagonize chemotherapy-induced cell death through autophagy induction and down-regulation of p62/sequestosome 1, J. Biol. Chem. 286 (46) (2011 Nov 18) 40002–40012.
[47] C. Petigny-Lechartier, C. Duboc, A. Jebahi, M.H. Louis, E. Abeilard, C. Denoyelle, et al., The mTORC1/2 inhibitor AZD8055 strengthens the efficiency of the MEK inhibitor trametinib to reduce the Mcl-1/[Bim and Puma] ratio and to sensitize ovarian carcinoma cells to ABT-737, Mol. Cancer Ther. 16 (1) (2017 Jan) 102–115.
[48] I.K. Zervantonakis, C. Iavarone, H.Y. Chen, L.M. Selfors, S. Palakurthi, J.F. Liu, et al., Systems analysis of apoptotic priming in ovarian cancer identifies vulnerabilities and predictors of drug response, Nat. Commun. 8 (1) (2017 Aug 28) 365,017-00263-7.
[49] C. Iavarone, I.K. Zervantonakis, L.M. Selfors, S. Palakurthi, J.F. Liu, R. Drapkin, et al., Combined MEK and BCL-2/XL inhibition is effective in high-grade serous ovarian cancer patient-derived xenograft models and BIM levels are predictive of responsiveness, Mol. Cancer Ther. 18 (3) (2019 Mar) 642–655.
[50] Z.A. Wainberg, M. Alsina, H.P. Soares, I. Brana, C.D. Britten, G. Del Conte, et al., A multi-arm phase I study of the PI3K/mTOR inhibitors PF-04691502 and gedatolisib (PF-05212384) plus irinotecan or the MEK inhibitor PD-0325901 in advanced cancer, Target. Oncol. 12 (6) (2017 Dec) 775–785.
[51] A.M. Schram, L. Gandhi, M.M. Mita, L. Damstrup, F. Campana, M. Hidalgo, et al., A phase Ib dose-escalation and expansion study of the oral MEK inhibitor pimasertib and PI3K/MTOR inhibitor voxtalisib in patients with advanced solid tumours, Br. J. Canc. 119 (12) (2018 Dec) 1471–1476.
[52] J.M. Del Campo, M. Birrer, C. Davis, K. Fujiwara, A. Gollerkeri, M. Gore, et al., A randomized phase II non-comparative study of PF-04691502 and gedatolisib (PF-05212384) in patients with recurrent endometrial cancer, Gynecol. Oncol. 142 (1) (2016 Jul) 62–69.
[53] J.E. Grilley-Olson, P.L. Bedard, A. Fasolo, M. Cornfeld, L. Cartee, A.R. Razak, et al., A phase Ib dose-escalation study of the MEK inhibitor trametinib in combination with the PI3K/mTOR inhibitor GSK2126458 in patients with advanced solid tumors, Investig. New Drugs 34 (6) (2016 Dec) 740–749.
[54] D.S. Hong, S.M. Sebti, R.A. Newman, M.A. Blaskovich, L. Ye, R.F. Gagel, et al., Phase I trial of a combination of the multikinase inhibitor sorafenib and the farnesyltransferase inhibitor tipifarnib in advanced malignancies, Clin. Cancer Res. 15 (22) (2009 Nov 15) 7061–7068.
[55] R. Dummer, M. Beyer, K. Hymes, M.T. Epping, R. Bernards, M. Steinhoff, et al., Vorinostat combined with bexarotene for treatment of cutaneous T-cell lymphoma: in vitro and phase I clinical evidence supporting augmentation of retinoic acid receptor/retinoid X receptor activation by histone deacetylase inhibition, Leuk. Lymphoma 53 (8) (2012 Aug) 1501–1508.
[56] D. Gomez-Almaguer, R. Saldana-Vazquez, L. Tarin-Arzaga, M.A. Herrera-Rojas, A. Vazquez-Mellado de Larracoechea, O.G. Cantu-Rodriguez, et al., Combination of low-dose imatinib plus nilotinib for the treatment of chronic-phase chronic myeloid leukaemia after imatinib failure, Hematology 21 (7) (2016 Aug) 411–414.